Wei Zhang,[1] Mengrui Wu,[2] Teayoun Kim,[3] Ravi H. Jariwala,[1] W. John Garvey,[1] Nanlan Luo,[1] Minsung Kang,[1] Elizabeth Ma,[1] Ling Tian,[1] Dennis Steverson,[1] Qinglin Yang,[1] Yuchang Fu,[1] and W. Timothy Garvey[1,4]

Skeletal Muscle TRIB3 Mediates Glucose Toxicity in Diabetes and High-Fat Diet–Induced Insulin Resistance

Diabetes 2016;65:2380–2391 | DOI: 10.2337/db16-0154

PATHOPHYSIOLOGY

In the current study, we used muscle-specific TRIB3 overexpressing (MOE) and knockout (MKO) mice to determine whether TRIB3 mediates glucose-induced insulin resistance in diabetes and whether alterations in TRIB3 expression as a function of nutrient availability have a regulatory role in metabolism. In streptozotocin diabetic mice, TRIB3 MOE exacerbated, whereas MKO prevented, glucose-induced insulin resistance and impaired glucose oxidation and defects in insulin signal transduction compared with wild-type (WT) mice, indicating that glucose-induced insulin resistance was dependent on TRIB3. In response to a high-fat diet, TRIB3 MOE mice exhibited greater weight gain and worse insulin resistance in vivo compared with WT mice, coupled with decreased AKT phosphorylation, increased inflammation and oxidative stress, and upregulation of lipid metabolic genes coupled with downregulation of glucose metabolic genes in skeletal muscle. These effects were prevented in the TRIB3 MKO mice relative to WT mice. In conclusion, TRIB3 has a pathophysiological role in diabetes and a physiological role in metabolism. Glucose-induced insulin resistance and insulin resistance due to diet-induced obesity both depend on muscle TRIB3. Under physiological conditions, muscle TRIB3 also influences energy expenditure and substrate metabolism, indicating that the decrease and increase in muscle TRIB3 under fasting and nutrient excess, respectively, are critical for metabolic homeostasis.

Insulin resistance plays a major role in the pathophysiology of type 2 diabetes mellitus (T2DM) and involves impaired insulin-stimulated glucose uptake into skeletal muscle. Patients with metabolic syndrome and/or prediabetes are insulin resistant; however, as glucose tolerance deteriorates into overt T2DM, the superimposition of hyperglycemia worsens overall insulin resistance. This latter component of insulin resistance is known as glucose-induced insulin resistance or glucose toxicity (1–4). Intensive glycemic control, whether by weight loss (5), sulfonylureas (6,7), or insulin therapy (2), can reverse glucose-induced insulin resistance, and the resulting increase in whole-body insulin sensitivity is paralleled by increased glucose transport rates in adipocytes (8) and skeletal muscle (5). Likewise, patients with type 1 diabetes in poor glycemic control exhibit insulin resistance that can be reversed by intensified insulin therapy (9). Rats made diabetic by streptozotocin (STZ) exhibit a reduction in insulin-stimulated glucose transport in muscle and fat, which can be reversed by euglycemia induced by exogenous insulin or by promotion of glycosuria with phlorizin (10,11). Finally, multiple in vitro studies demonstrate direct effects of glucose to impair insulin-stimulated glucose transport in perfused target tissues (12) and cultured cell systems (13,14). Thus, a large body of data supports the contention that glucose per se can induce desensitization of insulin's action to stimulate glucose uptake.

The mechanism by which glucose induces insulin resistance involves decreased activity of the glucose transport effector system and impaired translocation of intracellular GLUT4 to the cell surface in adipocytes and skeletal muscle (13,15,16). Furthermore, Marshall and colleagues (17–20) have shown that the ability of glucose to regulate its own

[1]Department of Nutrition Sciences, University of Alabama at Birmingham, Birmingham, AL
[2]Department of Molecular & Cellular Pathology, University of Alabama at Birmingham, Birmingham, AL
[3]Department of Medicine-Endocrinology, Diabetes & Metabolism, University of Alabama at Birmingham, Birmingham, AL
[4]Birmingham Veterans Affairs Medical Center, Birmingham, AL

Corresponding authors: W. Timothy Garvey, garveyt@uab.edu, and Wei Zhang, siweizh@uab.edu.

Received 1 February 2016 and accepted 26 April 2016.

This article contains Supplementary Data online at http://diabetes.diabetesjournals.org/lookup/suppl/doi:10.2337/db16-0154/-/DC1.

uptake depends on its intracellular metabolism via the hexosamine biosynthetic pathway (HBP). The HBP provides the capacity for *O*-linked glycosylation of protein, which can alter functional activity of enzymes and transcription factors. However, the actual downstream mechanisms by which glucose metabolic flux through the HBP mediates insulin resistance and diminished activity of the GLUT system activity in diabetes remain unknown despite more than two decades of study.

Tribbles homolog 3 (TRIB3), also named as TRB3, NIPK, SIKP3, has been identified as a pseudokinase that inhibits AKT activity by physically occupying its phosphorylation site (21). Expression of TRIB3 has been associated with various signals, such as endoplasmic reticulum stress and nutrient availability, in pancreatic β-cells, liver, adipose tissue, and skeletal muscle (21–23). Overexpression of TRIB3 in mouse liver led to decreased glycogen synthesis, increased hepatic glucose output, and higher blood glucose levels (21). Mice with TRIB3 overexpression in adipose tissue displayed enhanced fatty acid oxidation and were protected from obesity induced by a high-fat diet (HFD) (24).

Our interest in TRIB3 was first initiated when we used high-density cDNA microarrays to identify TRIB3 as an upregulated gene in skeletal muscle from patients with T2DM (25,26). In several subsequent studies, we demonstrated that TRIB3 protein levels were elevated in skeletal muscle from hyperglycemic rodent models and from patients with T2DM in a manner that was positively correlated with fasting glucose level, that TRIB3 levels were regulated by media glucose concentrations in L6 myotubes, and that overexpression of TRIB3 blocked insulin-stimulated GLUT rates (27). Our prior studies in cultured cells also demonstrated that glucose-induced insulin resistance is dependent upon induction of TRIB3 in a process that requires metabolism through the HBP (28). These data indicated that TRIB3 could have a pivotal role in regulating glucose homeostasis and could mediate insulin resistance in diabetes. In the current study, we investigated the effects of muscle-specific overexpression or knockout of TRIB3 on whole-body metabolism and tested the hypothesis that TRIB3 mediates glucose-induced insulin resistance (glucose toxicity) in diabetes.

RESEARCH DESIGN AND METHODS

Generation of Genetically Manipulated Mice

To generate transgenic mice with overexpression of TRIB3 in skeletal muscle, a floxed stop CAT gene was inserted between the CAG promoter (cytomegalovirus early enhancer/chicken β-actin promoter) sequence and the cDNA of human TRIB3 (Fig. 1*A*). Transgenic animals will not express the TRIB3 transgene until Cre is presented, leading to excision of the floxed stop CAT gene. For generating TRIB3 muscle knockout mice, a floxed TRIB3 potential knockout mouse model was purchased from the European Conditional Mouse Mutagenesis Program. The flippase (FLP) recombinase target (FRT) flanked-sequence in TRIB3 potential knockout mice was removed via crossing with FLP mice containing FLP recombinase (The Jackson Laboratory). These mice were then bred with our muscle-specific Cre mice (B6.Cg-Tg[ACTA1-cre]79Jme/J; The Jackson Laboratory) to generate muscle-specific TRIB3 knockout mice. For the high fat–feeding experiment, control and transgenic mice at age 8 weeks were fed with the HFD (60% kcals from fat; Research Diets Inc., New Brunswick, NJ) for up to 24 weeks. All animal procedures were approved by the Animal Resources Program Institutional Animal Care and Use Committee at the University of Alabama at Birmingham (UAB).

Diabetic Mice Study

At 20 weeks of age, a daily dose of STZ (50 mg/kg body weight [BW] in 10 mmol/L sodium citrate buffer, pH 4.5) was injected intraperitoneally for 5 days. Control animals receive only the vehicle buffer. Animals were considered diabetic when fasting blood glucose was >250 mg/dL measured using a GLUCOCARD Vital glucometer (Arkray). Insulin tolerance tests (ITT) were conducted multiple times in control and TRIB3-manipulated mice before and after induction of hyperglycemia. Animals were killed at 7 weeks of diabetes. Serum was collected and tissue samples were snap-frozen in liquid nitrogen and stored at −80°C for later use.

Glucose Tolerance Tests and ITT

Glucose tolerance tests and ITT were performed in wild-type (WT) and genetically manipulated mice under multiple physiological conditions, including normal chow diet feeding, HFD feeding, and STZ-induced diabetes. To assess glucose tolerance, animals were first fasted overnight and then given an intraperitoneal injection of glucose solution (100 g of glucose per liter; 1 g/kg BW). Mouse tail blood drops were taken, and glucose concentrations were determined at baseline (before injection) and at 30, 60, 90 and 120 min after injection using the GLUCOCARD Vital glucometer. To determine insulin tolerance, mice were fasted for 6 h (8 A.M.–2 P.M.) and then administered an intraperitoneal injection of insulin solution (Humalog, 0.3–0.5 units/kg BW). Glucose levels in response to the insulin injection were measured in blood samples collected as described above for the glucose tolerance test.

Body Composition Analysis

Fat and lean mass were measured in vivo using the quantitative EchoMRI 3-in-1 MRI system (Echo Medical Systems, Houston, TX) in the UAB Diabetes Research Center's Animal Physiology Core.

Indirect Calorimetry Analysis

Total energy expenditure (TEE), respiratory exchange ratio (RER), and physical activity were measured using an 8-cage indirect calorimetry system (CaloSys; TSE Systems, Bad Homburg, Germany) in the Animal Physiology Core. Mice were individually kept in airtight plastic cages with ad libitum access to food and water and a continuous flow of air was maintained through all cages. Mice were

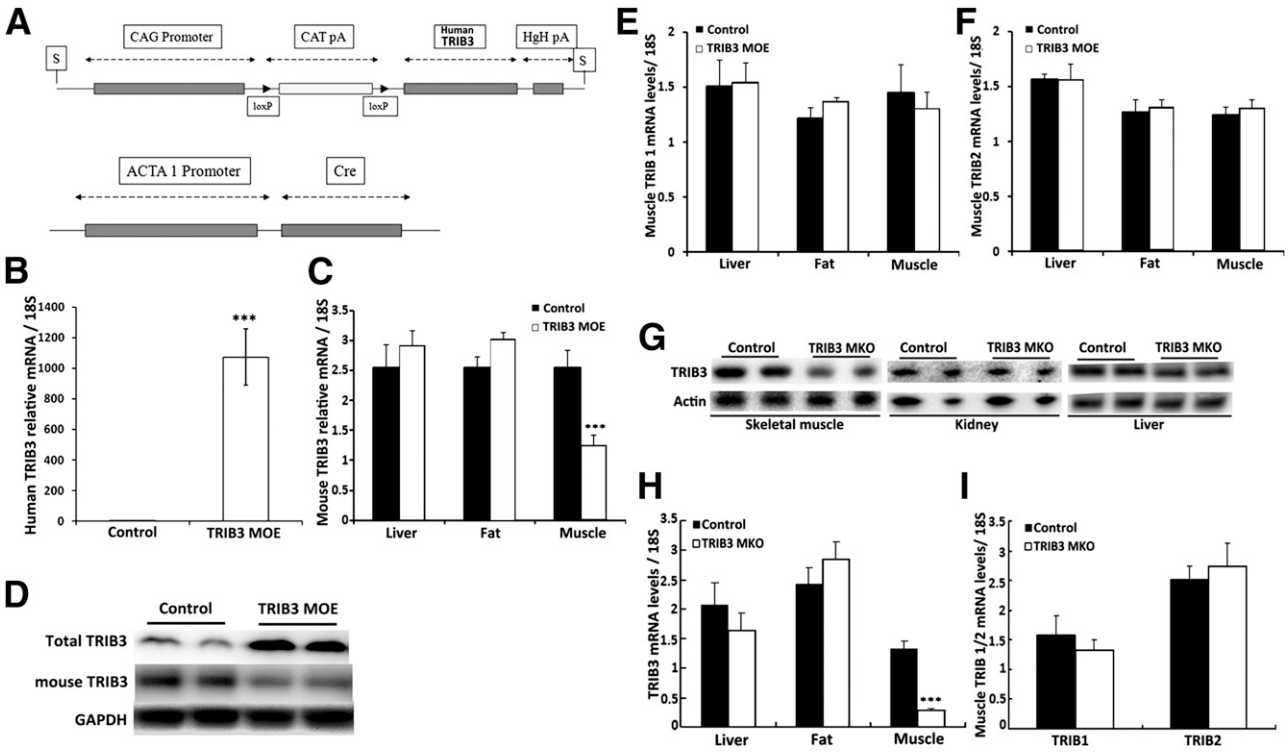

Figure 1—Expression of TRIB family in TRIB3 MOE and TRIB3 MKO mice. *A*: Construct map of loxP and Cre mice. *B–D*: Real-time PCR and Western blot confirm overexpression of human TRIB3 and suppressed endogenous mouse TRIB3 expression in skeletal muscle of TRIB3 MOE mice. *E* and *F*: Expressions of TRIB1 and TRIB2 in liver, fat, and muscle tissues of TRIB3 MOE mice. *G* and *H*: Western blot and real-time PCR confirm specific knockout of TRIB3 in skeletal muscle in TRIB3 MKO mice. *I*: TRIB1/2 expressions in skeletal muscle of TRIB3 MKO mice (n = 6–7). Data are presented as the means ± SEM. ***P < 0.001 vs. control group by the Student t test.

acclimated to the cages for 48 h before the 22-h measurement period. TEE was calculated for 22 h and presented as value per 24 h. Resting energy expenditure was calculated as the average of the three lowest 18-min periods during the measurement.

Insulin-Stimulated Glucose Oxidation Assay

Intact muscle oxidation assay was performed as previously described (29). Extensor digitorum longus muscles were excised from the dead mice and incubated with 700 μL of Krebs-Ringer phosphate buffer containing 0.1 μCi/mL of BSA-conjugated [^{14}C]palmitate or [^{14}C]glucose in sealed 14-mL tubes with center wells containing 1N NaOH at 37°C for 1 h. After incubation, 400 μL of 3.5 mol/L $HClO_4$ was injected into the media and incubated at 50°C for 3 h to capture oxidized substrates to NaOH. The radioactivity was measured by scintillation counter.

RNA Isolation and Expression Analysis

Tissue samples were homogenized in TRIzol reagent (Invitrogen), and total RNA was extracted using RNeasy columns with DNase I treatment (Qiagen, Valenica, CA). cDNA was synthesized by VILO kit (Invitrogen), following the manufacturer's instructions. The StepOnePlus 96-well machine (Applied Biosystems, Foster City, CA) was applied for real-time quantitative PCR analysis. PCR products were detected using SYBR Green and normalized to 18S ribosomal RNA, using specific oligonucleotides (primer sequences are available at request).

Protein Isolation and Immunoblot Analysis

For insulin stimulation, animals were given an intraperitoneal injection of insulin solution (Humalog, 0.5 units/kg BW) 30 min before being anesthetized for blood and tissue collection. Tissue proteins were extracted in lysis buffer containing 50 mmol/L Tris-HCl (pH 7.5), 150 mmol/L NaCl, 0.1% SDS, 1% Na deoxycholate, 1% NP-40, 10 mmol/L NaF, 5 mmol/L Na_3VO_4, 2 mg/mL pepstatin, 2 mmol/L phenylmethylsulfonyl fluoride, 1 mmol/L dithiothreitol, 20 μg/mL leupeptin, and 10 μg/mL aprotinin. The bicinchoninic acid kit (Sigma-Aldrich, St. Louis, MO) was used for quantifying protein concentrations.

Proteins were separated by SDS-PAGE for subsequent Western blotting. Primary antibodies: phosphorylated (p)-AKT Ser473 (#9271), p-AKT Thr308(#9275), AKT (#9272), p-glycogen synthase (GS) kinase (GSK)-3 α/β (Ser21/9) (#9331), GSK3 α/β (#5676), p-AMP-activated protein kinase α (AMPK-α) (#2531), and AMPK-α (#2532) were from Cell Signaling Technology (Danvers, MA), anti-AS160 antibody (rabbit p-Ab, #07-741) was from Upstate (Lake Placid, NY). Anti–p-GS (Thr642, rabbit; #441071G) was purchased from Biosource (Camarillo, CA). TRIB3

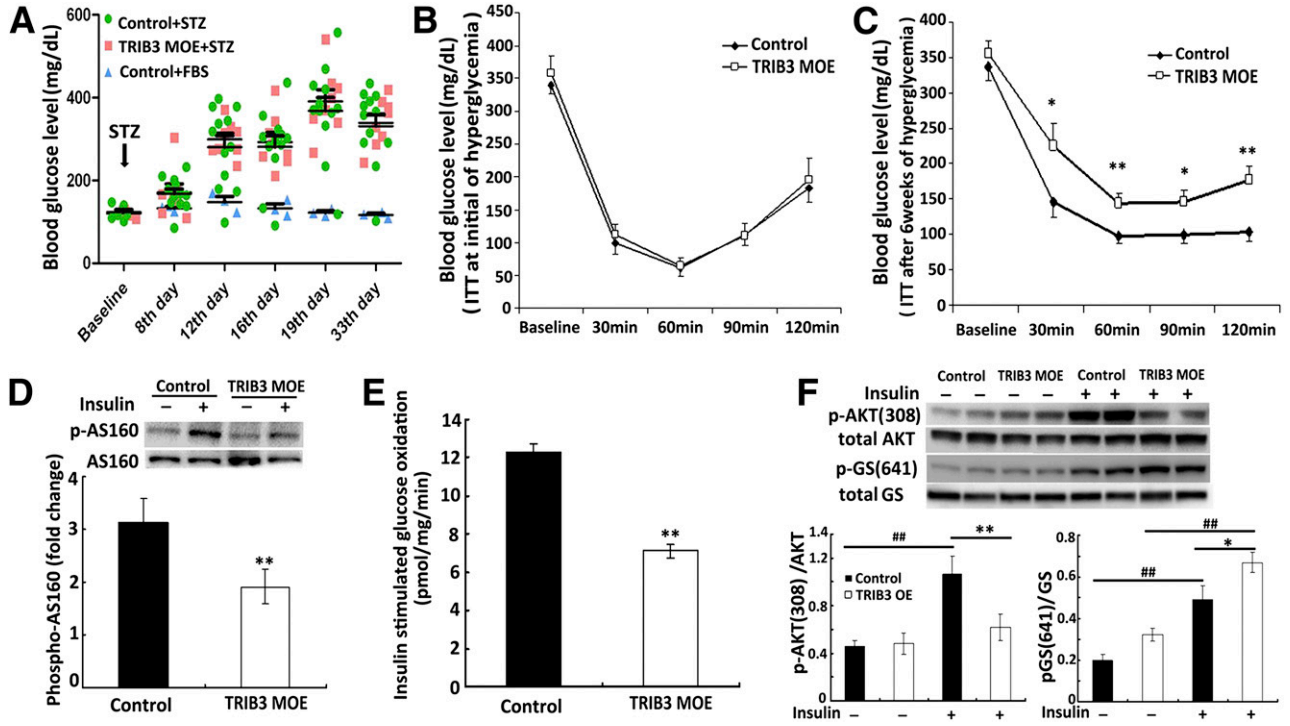

Figure 2—High-glucose–induced insulin resistance in TRIB3 MOE mice. *A*: Induction of hyperglycemia in control and TRIB3 MOE 20-week-old male mice (n = 8–12) by intraperitoneal injection of STZ (50 mg/kg BW for 5 consecutive days). *B*: ITTs (Humalog, 0.3 units/kg BW) were done at the very initial hyperglycemia (day 7), showing similar insulin sensitivity between groups. *C*: ITT (Humalog, 0.3 units/kg BW) conducted after 6 weeks of hyperglycemia. *D*: Skeletal muscle of TRIB3 MOE mice showed impaired insulin-stimulated p-AS160 compared with control mice. *E*: After 6 weeks' exposure to hyperglycemia, insulin-stimulated glucose oxidation rates were significantly decreased in the skeletal muscle of TRIB MOE mice compared with hyperglycemic control mice. *F*: Decreased insulin-stimulated p-AKT(308) in skeletal muscle of hyperglycemic TRIB3 MOE mice and increased p-GS (641) in TRIB3 MOE muscle. Data are means ± SEM. $^{*}P < 0.05$, $^{**}P < 0.01$ vs. the control group, and $\#\#P < 0.01$ vs. corresponding control by the Student t test and two-way ANOVA.

antibodies were from Calbiochem (Damstadt, Germany) and Santa Cruz Biotechnology (Dallas, TX). Anti–*O*-N-acetylglucosamine (GlcNAc) antibody was from Cell Signaling (CTD110.6 mouse monoclonal antibody). Horseradish peroxidase-conjugated secondary antibodies were from Santa Cruz Biotechnology. Images were captured by using enhanced chemiluminescence (Pierce) on a ChemiDoc XRS imager (BioRad, Hercules, CA), and Image Lab software (BioRad) was subsequently used for quantification.

Measurement of Insulin, Cholesterol, and Triglyceride Concentrations in Mouse Plasma

The insulin levels in mouse plasma were measured using an ultrasensitive mouse insulin ELISA kit from Crystal Chem (Downers Grove, IL) according to the manufacturer's protocols. The concentrations of cholesterol and triglyceride in mouse plasma were determined using enzymatic colorimetric assays (Wako, Richmond, VA) according to the manufacturer's protocols.

Statistical Analysis

Experimental results are shown as the mean ± SEM. Statistical analyses were conducted using the unpaired Student t test assuming unequal variance or using one-way or two-way ANOVA.

RESULTS

Generation of Genetically Manipulated Mouse Models

To determine the contribution of TRIB3 to glucose-induced insulin resistance in vivo, we generated mice with muscle-specific TRIB3 overexpression (MOE) and knockout (MKO). As shown in Fig. 1, MOE mice highly expressed the human TRIB3 transgene in skeletal muscle coupled with an ~50% reduction in endogenous mouse TRIB3 (Fig. 1*B* and *C*), resulting in a four- to fivefold increase in total muscle TRIB3 protein (i.e., human and mouse TRIB3) (Fig. 1*D*). TRIB3 MOE did not affect levels of TRIB1 or TRIB2 in liver, adipose tissue, and skeletal muscle (Fig. 1*E* and *F*). TRIB3 MKO resulted in an 80% decrease in TRIB3 mRNA and protein in skeletal muscle (Fig. 1*E* and *H*). Suppression of TRIB3 expression in muscle did not result in alteration in expression of TRIB3 in liver and fat (Fig. 1*H*) and did not affect levels of TRIB1 or TRIB2 in muscle (Fig. 1*I*).

The Pathophysiological Role of Muscle TRIB3 as a Mediator of Glucose-Induced Insulin Resistance in Diabetes

Our previous studies implicated TRIB3 as a mediator for glucose-induced insulin resistance (27,28). To study whether TRIB3 is responsible for glucose-induced insulin

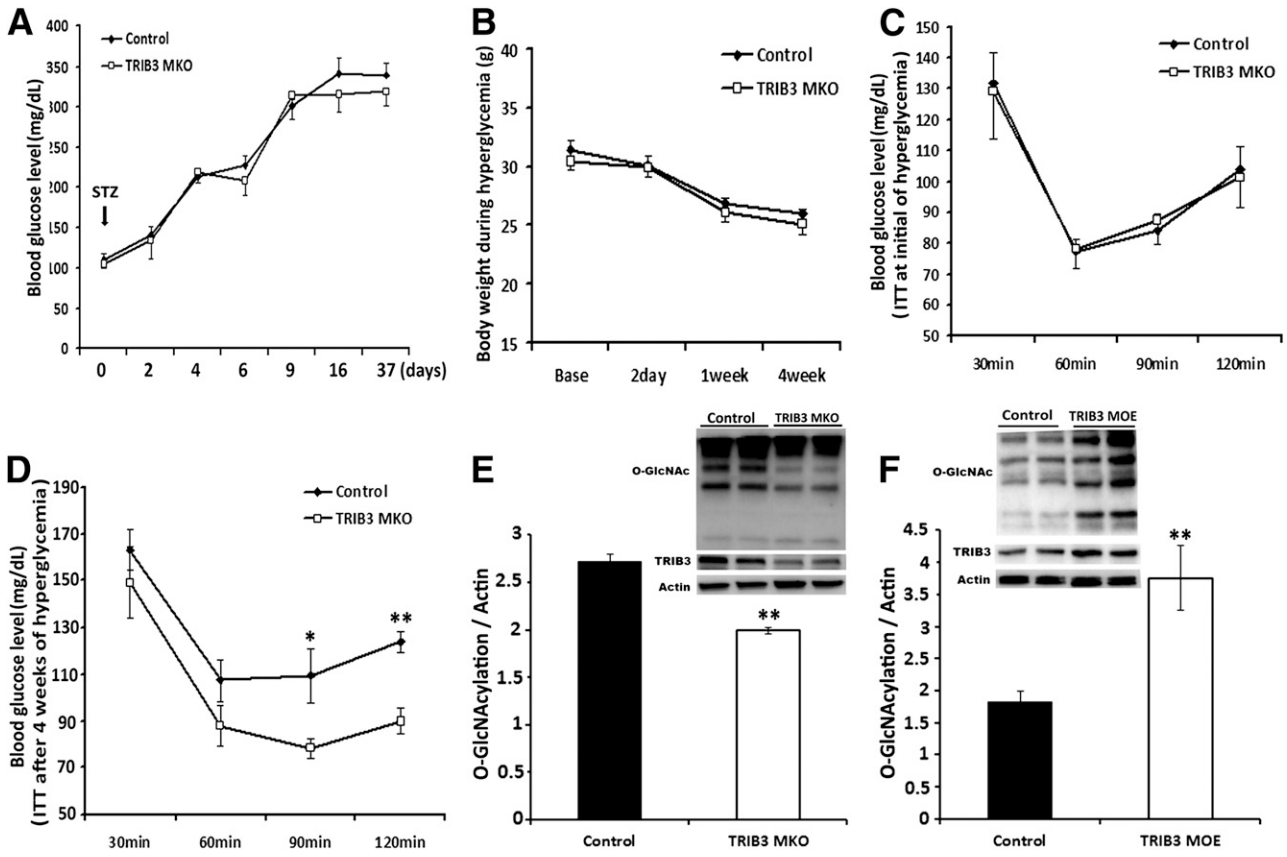

Figure 3—TRIB3 MKO mice were protected from high-glucose–induced insulin resistance in diabetes. *A*: Induction of hyperglycemia in control and TRIB3 MKO 20-week-old male mice (n = 8–12) by intraperitoneal injection of STZ (50 mg/kg BW for 5 consecutive days). *B*: Similar weight loss between control and TRIB3 MKO mice during hyperglycemia. *C*: ITTs (Humalog, 0.3 units/kg BW) were done at the very initial beginning of hyperglycemia (day 7), showing similar insulin sensitivity between groups. *D*: ITT (Humalog, 0.3 units/kg BW) repeated after 4 weeks of hyperglycemia in TRIB3 MKO mice and control mice. *E* and *F*: Western blot analysis of total protein *O*-GlcN acylation in skeletal muscle of TRIB3 MKO and TRIB3 MOE diabetic mice. Data are means ± SEM. $^*P < 0.05$ and $^{**}P < 0.01$ vs. control group by the Student t test and two-way ANOVA.

resistance in vivo in the setting of diabetes, we used STZ injection to induce hyperglycemia in control and TRIB3 MOE mice. Overt diabetes was fully developed after 12 days after the STZ injection and sustained over 33 days of observation (Fig. 2*A*). No significant difference in the degree of hyperglycemia was observed between control and TRIB3 MOE mice. Insulin sensitivity assessed by ITT early in the course of diabetes on day 7 was similar in comparing the two groups of mice (Fig. 2*B*), but after 6 weeks with longer duration of diabetes, TRIB3 MOE mice were more insulin resistant and exhibited significantly impaired response to insulin than the WT controls (1-h ITT glucose: 137 ± 13 vs. 90 ± 6 mg/dL, 2-h ITT glucose: 170 ± 18 vs. 97 ± 13 mg/dL, $P < 0.01$) (Fig. 2*C*). Insulin-stimulated p-AS160 was significantly reduced in TRIB3 MOE mice (Fig. 2*D*), which is associated with impaired translocation of GLUT (30). In addition, insulin-stimulated glucose oxidation (Fig. 2*E*) and p-AKT (Fig. 2*F*) was significantly decreased in skeletal muscle of TRIB3 MOE mice, whereas p-GS was increased, which would have the effect to decrease glycogen synthesis/storage in skeletal muscle of TRIB3 MOE mice (Fig. 2*F*). The above findings collectively suggested that hyperglycemia produced a greater degree of insulin resistance systemically and in skeletal muscle in TRIB3 MOE mice, supporting the hypothesis that TRIB3 acts as a mediator of glucose-induced insulin resistance in diabetes.

To further confirm a role for TRIB3 in glucose-induced insulin resistance in vivo, we used the same STZ injection protocol to induce hyperglycemia in control and TRIB3 MKO mice and monitored the development of insulin resistance during diabetes by serial ITT. STZ injection induced similar levels of hyperglycemia and changes in BW in control and TRIB3 MKO mice, without significant intergroup differences (Fig. 3*A* and *B*). As shown in Fig. 3*C*, ITT conducted at the initiation of diabetes (day 7) displayed very similar insulin sensitivity between control and TRIB3 MKO mice. However, after 4 weeks of hyperglycemia, TRIB3 MKO mice were significantly protected from development of insulin resistance compared with control mice (1-h ITT glucose: 87 ± 8 vs. 107 ± 8 mg/dL,

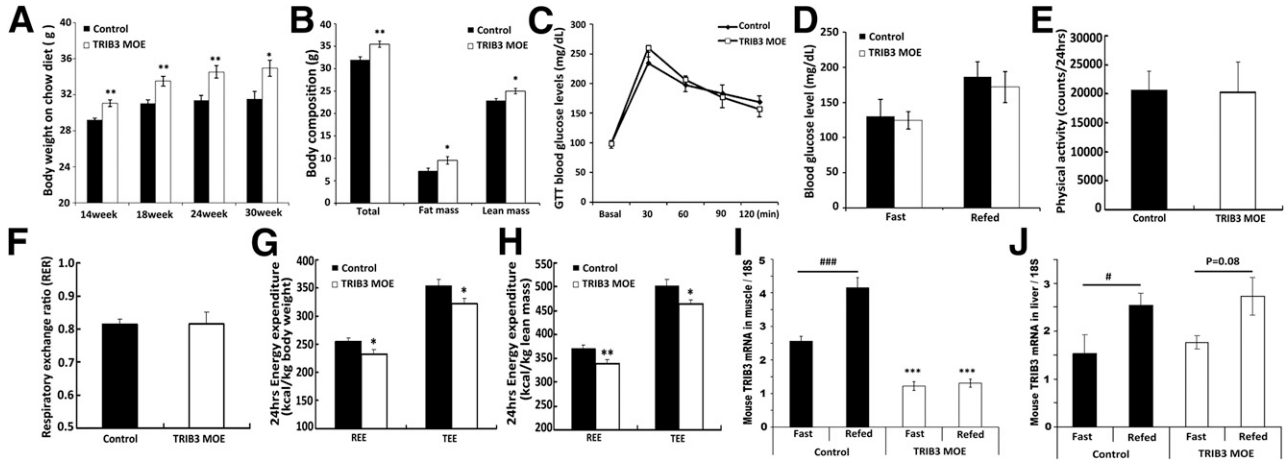

Figure 4—Effects of chow-diet feeding on control and TRIB3 MOE mice. *A*: TRIB3 MOE mice exhibited higher BW gain. *B*: Quantitative MRI test shows increases of fat mass and lean mass contributed to gain of BW in TRIB3 MOE mice. *C* and *D*: No significant differences were observed on glucose tolerance test (GTT) and blood glucose levels in mice fed the chow diet. *E*: Physical activity for 24 h was similar between control and TRIB3 MOE mice. *F*: RER was similar between control and TRIB3 MOE mice. *G* and *H*: TRIB3 MOE mice exhibited decreased 24-h energy expenditure normalized by total BW or total body lean mass. *I*: Endogenous mouse TRIB3 expressions were suppressed in skeletal muscle under fasting and feeding conditions, In addition, physiological regulation of endogenous mouse TRIB3 expression by nutrient availability was blunted in skeletal muscle of TRIB3 MOE mice. *J*: Expression and nutrient regulation of endogenous mouse TRIB3 in liver were not affected in TRIB3 MOE mice. Data are the means ± SEM (n = 7–12). *P < 0.05, **P < 0.01, and ***P < 0.001 vs. control group by Student t test or two-way ANOVA; #P < 0.05, ###P < 0.001 vs. Fast control group.

$P < 0.05$; 2-h ITT glucose: 90 ± 5 vs. 139 ± 16 mg/dL, $P < 0.01$) (Fig. 3*D*). The protection lasted until week 7 of hyperglycemia, when mice were killed for tissue collection. Our previous studies indicated that TRIB3 mediates glucose-induced insulin resistance via the HBP pathway in cultured cells (27,28); in the current study, protein *O*-GlcN acylation was significantly decreased in diabetic TRIB3 MKO mice and was increased in diabetic TRIB3 MOE mice (Fig. 3*E* and *F*). These findings support the hypothesis that glucose-induced insulin resistance in vivo is dependent upon muscle TRIB3 and that TRIB3 has a pathophysiological role in the glucose toxicity of diabetes.

The Physiological Role of Muscle TRIB3

In addition to the pathophysiological role of TRIB3 in the setting of sustained hyperglycemia, we previously demonstrated that TRIB3 expression was oppositely regulated in muscle and fat under physiological conditions of fasting and nutrient excess. Specifically, short-term fasting produced a decrease in TRIB3 mRNA and protein content in skeletal muscle associated with enhanced in vivo insulin sensitivity together with an increase in TRIB3 expression in adipose tissue. In addition, rats fed a Western diet for 1 week became insulin resistant associated with an increase in muscle TRIB3 combined with decreased expression in adipose tissue (23). On the basis of our studies in cultured cells (23,28), these changes would predictably promote increased glucose uptake in muscle coupled with a diminished emphasis on fuel storage in adipose tissue under fasting conditions and reduced substrate muscle uptake plus promotion of fuel storage in adipose during nutrient excess. We have now used our TRIB3 MOE and MKO mouse models to determine whether the regulatory changes in muscle TRIB3 levels do exert a primary effect to alter systemic metabolism.

Overexpression of TRIB3 in skeletal muscle did alter whole-body energy balance. TRIB3 MOE mice exhibited higher BW while being fed a normal chow diet (Fig. 4*A*), and quantitative MRI results indicated that the increase in weight was due to increments in fat mass and in lean mass (Fig. 4*B*). Despite a higher BW, glucose tolerance test and blood glucose levels were not significantly different between control and TRIB3 MOE mice (Fig. 4*C* and *D*). Indirect calorimetry demonstrated that TRIB3 MOE mice exhibited similar physical activity and RER as control mice (Fig. 4*E* and *F*); however, TRIB3 MOE mice had significantly decreased resting energy expenditure and TEE normalized to total BW (Fig. 4*G*) or total body lean mass (Fig. 4*H*), which would have contributed to higher weight gain in TRIB3 MOE mice. Overexpression of human TRIB3 in muscle also disrupted the physiological regulation of endogenous mouse TRIB3 to fasting. As we previously observed in rats (23), TRIB3 levels in WT mice were lower under fasting conditions but then increased in both muscle and liver upon refeeding (Fig. 4*I* and *J*). However, TRIB3 MOE mice lost the physiological responses to fasting and feeding (Fig. 4*I*), with reduced mouse TRIB3 levels in muscle under fasting conditions that were not altered upon refeeding. In contrast, the physiological regulation of mouse TRIB3 in liver with fasting and refeeding remained similar to that in control (Fig. 4*J*).

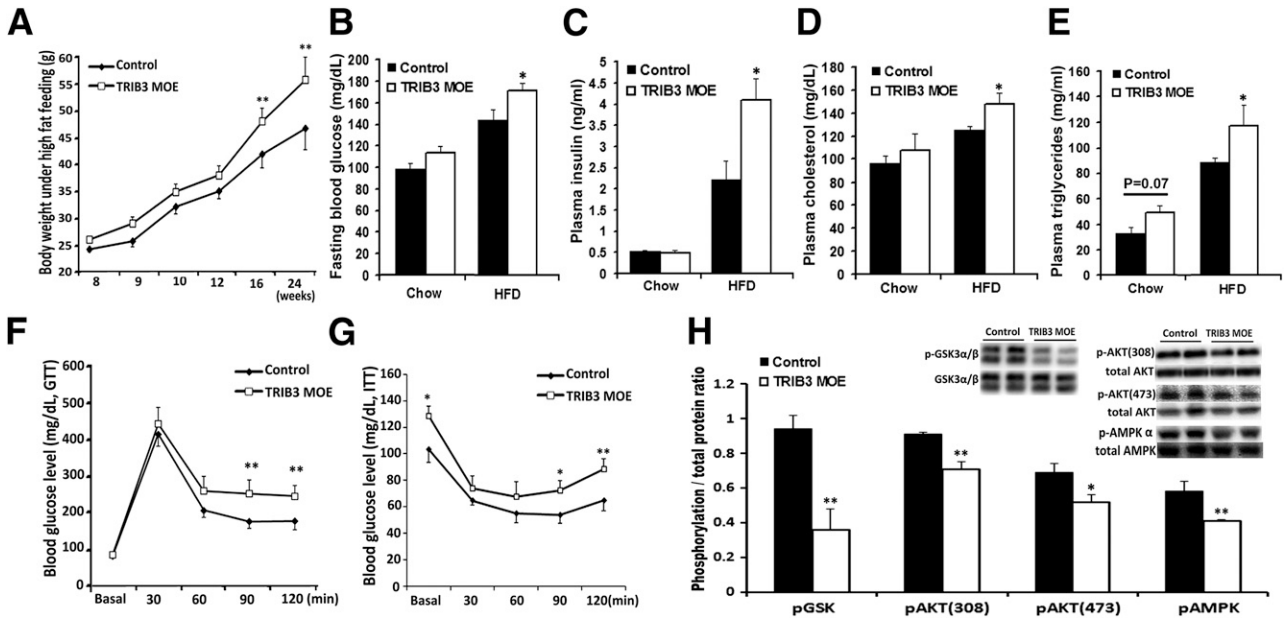

Figure 5—HFD feeding induced insulin resistance in TRIB3 MOE mice. *A*: TRIB3 MOE mice developed significantly heavier BW after 16 weeks of the HFD. Fasting glucose (*B*), insulin (*C*), cholesterol (*D*), and triglyceride (*E*) levels in control and TRIB3 MOE mice ($n = 6$). *F*: TRIB3 MOE mice exhibited significantly impaired glucose tolerance on glucose tolerance test (GTT; glucose 2 g/kg BW, i.p.) under high-fat feeding ($n = 7$). *G*: TRIB3 MOE mice developed significantly impaired insulin sensitivity as reflected by ITT (Humalog, 0.5 units/kg BW, i.p.; $n = 7$). *H*: Western blot analysis of insulin-signaling proteins in muscle tissue collected after 30 min of insulin injection (Humalog, 0.5 units/kg BW, i.p.; $n = 3$). HFD led to obviously impaired insulin signal transduction in skeletal muscle of TRIB3 MOE mice, including decreased p-GSK3 α/β, p-AKT(308), p-AKT (473), and p-AMPK-α ($n = 3$). Data are means ± SEM. $^*P < 0.05$ and $^{**}P < 0.01$ vs. control group by two-way ANOVA.

We then examined whether TRIB3 MOE affected metabolism under the condition of nutrient excess. With chronic HFD feeding for 16 weeks, TRIB3 MOE mice developed significantly higher BW (Fig. 5*A*), now accompanied by increased fasting blood glucose, plasma insulin, total cholesterol, and triglyceride levels (Fig. 5*B*–*E*). The HFD-fed TRIB3 MOE mice also exhibited impaired glucose tolerance and significantly higher insulin resistance compared with WT controls (Fig. 5*F* and *G*). Insulin-stimulated phosphorylation of GSK3 α/β, AKT^{308}, AKT^{473}, and AMPKα was substantially decreased in skeletal muscle of TRIB3 MOE mice, indicating impaired insulin signal transduction in muscle from the TRIB3 MOE mice (Fig. 5*H*).

To determine whether suppression of TRIB3 can protect against the development of insulin resistance under nutrient excess, we studied TRIB3 MKO and WT mice fed the HFD for 16 weeks. Despite similar BW gain between control and TRIB3 MKO mice (Fig. 6*A*), TRIB3 MKO mice exhibited lower fasting blood glucose correlated with decreased gluconeogenic gene (PEPCK) expression during fasting (Fig. 6*B* and *C*). TRIB3 MKO mice were also significantly protected from developing insulin resistance compared with WT controls (Fig. 6*D*). Insulin signal transduction was also better preserved in TRIB3 MKO mice, as reflected by higher insulin-stimulated p-GSK3 α/β, p-AKT^{308} and p-AKT^{473} in TRIB3 MKO muscle (Fig. 6*E*) compared with HFD-fed control mice. These observations confirmed that muscle-specific suppression of TRIB3 is protective against insulin resistance under chronic nutrient excess conditions (i.e., HFD).

Effects of Muscle TRIB3 on Inflammation, Oxidative Stress, and Substrate Metabolism

Together with more profound insulin resistance, the expression of multiple proinflammatory genes was significantly elevated in skeletal muscle of TRIB3 MOE mice fed the HFD compared with WT mice, including nuclear factor (NF)-κB, tumor necrosis factor α (TNF-α), MCP-1, and interleukin (IL) 6, whereas adiponectin (Adq) was significantly decreased (Fig. 7*A*). In addition to increased inflammatory markers, we also observed a marked increase in the expression of superoxide-generating NADPH oxidase-1 (NOX-1), but not NOX-2, in TRIB3 MOE muscle upon HFD feeding, indicating that TRIB3 could facilitate free radical formation under conditions of nutrient excess (Fig. 7*B*). These findings are consistent with previous reports showing that TRIB3 induces stress via the activating transcription factor 4 (ATF4)-CHOP pathway (31). Here, we also observed elevated transcription of ATF4 and CHOP in skeletal muscle of TRIB3 MOE mice fed normal chow (Fig. 7*C*). The HFD induced further increased expression of muscle CHOP in both TRIB3 MOE and control mice, although the increase was greater in control mice, perhaps reflecting feedback inhibition of TRIB3 on CHOP expression under these conditions, as has been previously

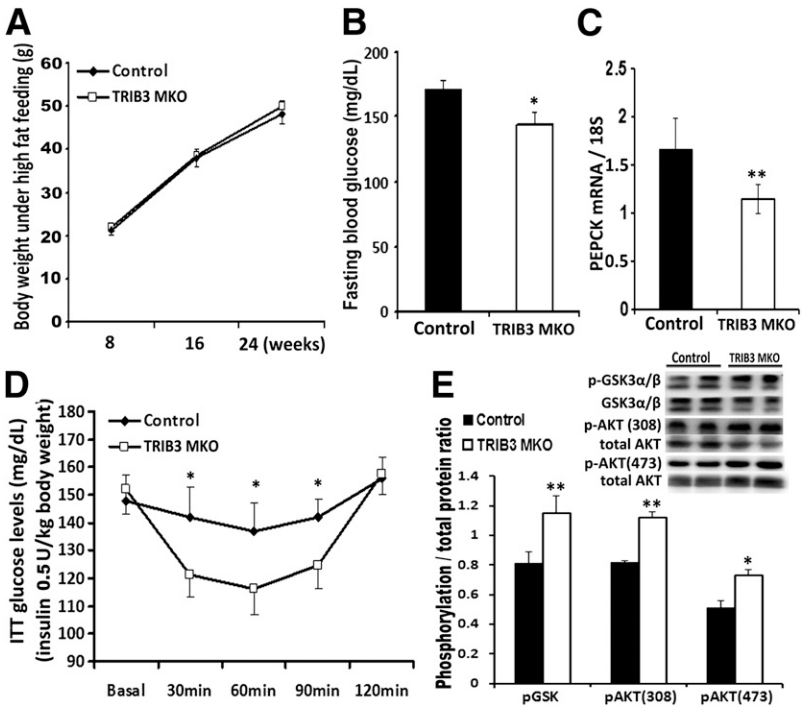

Figure 6—HFD feeding induced insulin resistance in TRIB3 MKO mice. *A*: Similar BW gain in control and TRIB3 MKO mice fed with the HFD for 16 weeks (n = 7–12). *B*. Compared with control mice, TRIB3 MKO mice had a significantly lower level of fasting blood glucose after being fed the HFD. *C*: Expression of gluconeogenic gene PEPCK in TRIB3 MKO and control mice under fasting. *D*: ITT (Humalog, 0.5 units/kg BW, i.p.) showed improved insulin sensitivity in TRIB3 MKO mice compared with control mice (n = 7). *E*: Western blot analysis of insulin signaling proteins in muscle tissue collected after 30 min of insulin injection (0.5 units/kg BW, i.p.), which showed increased p-GSK3 α/β and p-AKT (308) in skeletal muscle of TRIB3 MKO mice. Data are means ± SEM. *P < 0.05 and **P < 0.01 vs. control group by two-way ANOVA.

reported (32). Consistent with our hypothesis, TRIB3 MKO mice exhibited opposite effects on gene expression compared with what was observed in the TRIB3 MOE mice. In these TRIB3 MKO mice, greater insulin sensitivity was associated with reduced expression of proinflammatory cytokines, increased Adq, and suppression of NOX-1 and ATF4 (Fig. 7*D–F*).

Coupled with changes of cytokines, TRIB3 MOE mice exhibited significantly increased expression of macrophage genes in skeletal muscle, including adhesion G protein-coupled receptor E1(F4/80) and C-C chemokine receptor type 2 (CCR2) (Fig. 7*G*). In addition to the increase in pro-oxidative stress genes, TRIB3 MOE mice had significantly decreased expression of antioxidant genes, including catalase and glutathione peroxidase 1 and 4 (GPX1 and GPX4), whereas antioxidant genes were increased in TRIB3 MKO mice compared with WT, including catalase, superoxide dismutase 1(SOD1), and GPX1 (Fig. 7*I* and *J*). A paradoxical increase was found in Adq receptor 1 and 2 (AdR1/2) in muscle from TRIB3 MOE mice. AdR1 was unchanged in TRIB3 MKO mice, but expression of AdR2 was increased compared with WT (Fig. 7*G* and *H*). These findings consistently indicate that TRIB3 MOE mice were exposed to a higher level of oxidative stress with impaired antioxidation mechanisms.

TRIB3 MOE and MKO also altered expression of genes involved in pathways of fatty acid and glucose metabolism. Specifically, as shown in Fig. 8*A*, TRIB3 MOE mice exhibited higher expression of fatty acid oxidation genes and suppression of genes responsible for glucose metabolism. In contrast, TRIB3 MKO mice tended to upregulate genes for glucose metabolism and downregulate genes for fatty acid oxidation (Fig. 8*B*). These changes occurred without alterations in markers of mitochondrial mass, including COX1, COX2, UCP3, Cyt-C, and myogenin (data not shown). These data indicate that increased expression of TRIB3, observed under conditions of nutrient excess, may shift substrate oxidation in muscle away from glucose to emphasize fatty acid metabolism.

DISCUSSION

We have demonstrated that TRIB3 in intact mice has a pathophysiological role to mediate glucose-induced insulin resistance in diabetes and a physiological role to regulate metabolism and response to an HFD. Regarding the pathophysiological role, we previously demonstrated that TRIB3 mRNA and protein levels were upregulated (up to twofold) in skeletal muscle from patients with T2DM compared with insulin-sensitive individuals, and regression analysis revealed a positive correlation between TRIB3 muscle content and fasting blood glucose

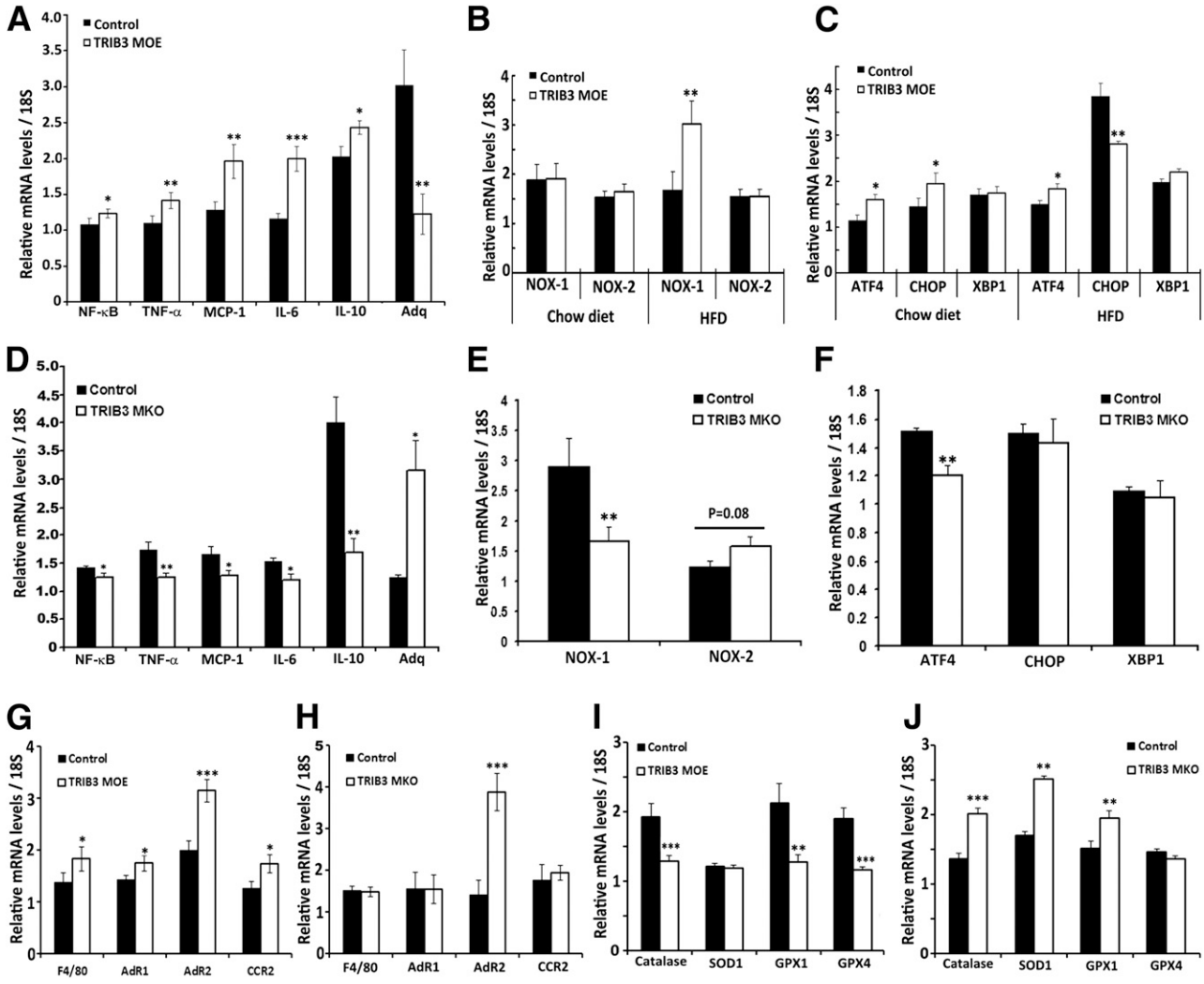

Figure 7—Opposite expressions of genes in inflammation, ROS production, and stress pathways in TRIB3 MOE and TRIB3 MKO mice. *A*: Increased NF-κB expression, elevated proinflammatory cytokines (TNF- α, MCP-1, IL-6, IL-10), and decreased anti-inflammatory cytokine Adq in skeletal muscle of TRIB3 MOE mice. *B*: ROS-producing gene NOX-1 but not NOX-2 expressions were significantly increased in skeletal muscle of TRIB3 MOE mice under HFD (nutrient excess condition). *C*: Increased ATF4-CHOP transcription in TRIB3 MOE mice, with a potential feedback inhibition on CHOP expression under the HFD condition. *D*: Decreased intramuscular inflammatory profile in TRIB3 MKO mice. *E*: ROS-producing gene NOX-1 was significantly decreased in TRIB3 MKO mice fed the HFD. *F*: Decreased endothelium reticulum stress gene ATF4 in skeletal muscle of TRIB3 MKO mice fed the HFD. *G* and *H*: Expressions of macrophage marker F4/80 and chemokine receptors (AdR1, AdR2, CCR2) in skeletal muscle of TRIB3 MOE and MKO mice fed the HFD. *I* and *J*: Expressions of critical antioxidants (catalase, SOD1, GPX1, and GPX4) in skeletal muscle of TRIB3 MOE and MKO mice fed the HFD. Real-time PCR was done in soleus muscle (n = 6). Data are means ± SEM. $^{*}P < 0.05$, $^{**}P < 0.01$, and $^{***}P < 0.001$ vs. control group by Student t test.

concentrations (25,33). In addition, high TRIB3 muscle expression was observed in multiple hyperglycemic rodent models of insulin resistance, such as rats injected with STZ (up to threefold), Zucker fatty rats, and *db/db* mice, compared with insulin-sensitive controls. Moreover, in vitro studies confirmed that high glucose levels induced TRIB3 expression in L6 muscle cells and that these higher levels of TRIB3 in turn impaired insulin-stimulated p-AKT and glucose uptake (27). The effects of high glucose to induce insulin resistance and augment TRIB3 expression were dependent upon the glucose metabolism via the HBP pathway, which is necessary for mediating glucose toxicity in diabetes (15,17,28). In cultured muscle cells, knockdown of TRIB3 inhibited and TRIB3 overexpression enhanced the ability of glucose flux via the HBP to induce insulin resistance (28). These observations led us to hypothesize that TRIB3 is an important systemic mediator of glucose toxicity in vivo.

To test the hypothesis that glucose-induced insulin resistance was dependent upon TRIB3 in diabetes, we generated mice with MOE and knockout. Insulin sensitivity was similar between control and TRIB3 MOE mice at the initiation of STZ diabetes, whereas after 6 weeks' exposure to hyperglycemia, TRIB3 MOE mice developed significantly worse insulin resistance than the WT mice, associated with decreased insulin-stimulated glucose

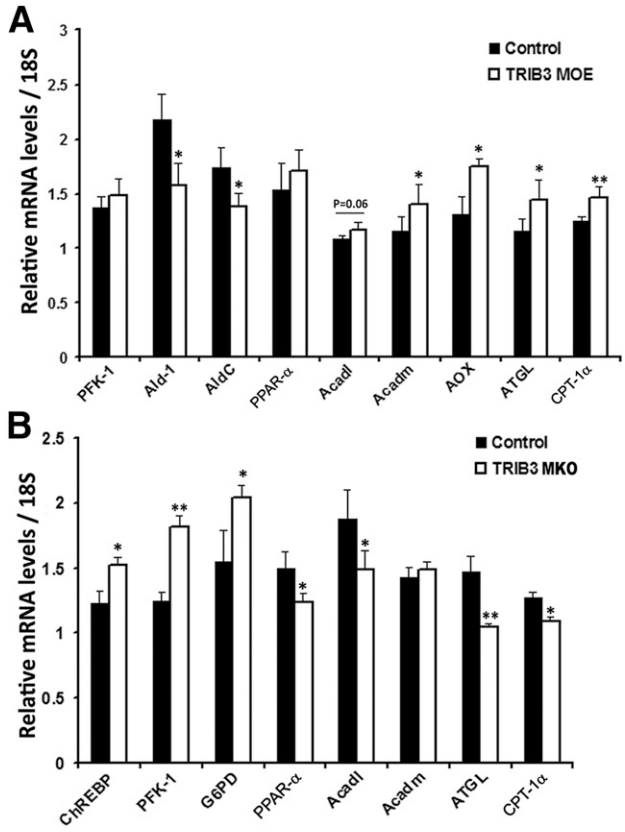

Figure 8—Substrate metabolism in TRIB3 MOE and TRIB3 MKO mice. *A*: Decreased glucose metabolic genes (aldolase A and aldolase C), plus multiple genes involved in fatty acid metabolism were significantly increased in TRIB3 MOE mice fed the HFD, including fatty acyl-CoA oxidase (AOX), median-chain acyl-CoA dehydrogenase (Acdam), long-chain acyl-CoA dehydrogenase (Acdal), adipose triglyceride lipase (ATGL), and carnitine palmitoyltransferase 1 α (CPT-1α). *B*: Increased glucose metabolic genes, including carbohydrate-responsive element–binding protein (ChREBP), phosphofructokinase 1 (PFK-1), and glucose-6-phosphate dehydrogenase (G6PD), and decreased fatty acid oxidation genes, including peroxisome proliferator–activated receptor α (PPAR-α), Acdal, ATGL, and CPT-1α in TRIB3 MKO mice fed the HFD. Data are means ± SEM (n = 6–8). *P < 0.05 and **P < 0.01 vs. control group by Student t test.

oxidation in muscle as well as impaired insulin signal transduction, including decreased p-AKT^{308}, p-GSK3 α/β, and p-AS160. In addition, TRIB3 MKO mice were protected from developing glucose-induced insulin resistance during hyperglycemia that was observed in diabetic WT mice, and changes in phosphorylation of insulin signal transduction molecules were prevented. *O*-GlcN acylation is the end product of glucose flux via the HBP pathway. In the current study, protein *O*-GlcN acylation was significantly decreased in diabetic TRIB3 MKO mice and increased in diabetic TRIB3 MOE mice, indicating that TRIB3 participated in the regulation of protein *O*-GlcN acylation. From this, we conclude that glucose-induced insulin resistance in diabetes is dependent upon muscle TRIB3.

By studying TRIB3 MOE and MKO, we were able to determine whether muscle TRIB3 has a physiological role to regulate metabolism in nondiabetic mice. We had previously shown in rats that TRIB3 is oppositely regulated in muscle and adipose tissue under conditions of fasting and nutrient excess (23). Because upregulation of TRIB3 in cultured muscle cells and adipocytes impairs insulin-stimulated glucose uptake and downregulation enhances insulin sensitivity, the regulatory changes were predicted to shift fuel from adipose tissue to muscle during fasting (TRIB3 upregulation in adipose and downregulation in muscle during fasting) and protect muscle against fuel overload while promoting storage in adipose during periods of nutrient excess (downregulation in adipose and upregulation in muscle while consuming a Western diet) (23,28). The current experiments in TRIB3 MOE and MKO mice demonstrate that muscle TRIB3 is indeed an important regulator of in vivo metabolism and that muscle TRIB3 is necessary for induction of insulin resistance during fasting and HFD feeding.

We observed that the TRIB3 MOE mice displayed greater weight gain while consuming the normal chow, without a change in body composition, as a result of lowered energy expenditure but that insulin sensitivity and glucose tolerance were unaffected compared with the WT mice. However, when challenged with the HFD, TRIB3 MOE mice developed a higher level of obesity and insulin resistance than the WT mice. Studies in muscle tissue demonstrated greater impairment in insulin signal transduction, substantially elevated levels of proinflammatory cytokines (NF-κB, IL-6, TNF-α, and MCP-1), and decreased Adq, which has been known as a beneficial adipocytokine with antidiabetic, anti-inflammatory, and antiatherogenic properties (34). By contrast, high-fat feeding failed to induce insulin resistance in TRIB3 MKO mice, and there was reduced expression of muscle cytokines and increased Adq as well as AdR2 levels relative to WT mice, consistent with a state of enhanced Adq action as part of the mechanisms for improved insulin sensitivity.

Coupled with augmented expression of inflammatory cytokines, TRIB3 MOE mice also displayed increased expression of chemokine receptors, including F4/80 and chemotactic receptor CCR2 in muscle, indicating chemotaxis of macrophages was part of the mechanism of increased inflammation. A paradoxical increase in muscle AdR1 and 2 was also noted in TRIB3 MOE mice, which could be due to upregulation in response to a decrease in Adq as we previously observed in adipocytes (35). In any event, previous studies have demonstrated that inflammation in muscle mediated by resident macrophages is associated with insulin resistance (36,37). The differential effects of TRIB3 MOE and MKO on cytokines and chemotactic factors likely partly explain the opposite effects on insulin sensitivity and the finding that HFD-induced insulin resistance is dependent on TRIB3.

NADPH oxidases (NOX1, NOX2, NOX4, and NOX5) represent an enzyme family that is directly involved in reactive oxygen species (ROS) production, which can augment ROS generation and inflammation and play an important role in vascular pathophysiology and insulin resistance (38,39). Induction of TRIB3 by ROS was previously reported in a study of kidney podocytes (40). In the current study, together with increased inflammation, TRIB3 overexpression in muscle also dramatically increased levels of the ROS-generating gene NOX-1 without affecting NOX-2. When insulin sensitivity is normal, circulating and intracellular fatty acid levels are low, and this is associated with reduced production of ROS via mitochondrial metabolism. In insulin resistance, however, elevated circulating and intracellular lipids lead to excessive production of ROS, which impairs mitochondrial function (41). In TRIB3 MOE, we observed decreased glucose oxidation and increased expression of genes involved in fatty acid oxidation in skeletal muscle, suggesting that TRIB3 can shift mitochondrial metabolism to favor oxidation of fatty acids. On the one hand, the increase in fat oxidation during nutrient excess condition (e.g., high-fat feeding) would produce more ROS, leading to inflammation and insulin resistance. On the other hand, TRIB3 MKO did not become insulin resistant during high-fat feeding associated with reduced NOX-1 expression and genes involved in fat oxidation.

Although somewhat speculative, this role of TRIB3 to modulate fat metabolism, ROS production, and insulin sensitivity via NOX-1 is consistent with data in vascular smooth muscle–specific transgenic mice overexpressing NOX-1. These mice exhibited increased vascular hypertrophy and hypertension due to ROS production (42), and deletion of NOX-1 exerted prominent antiatherosclerotic effects accompanied by reduced ROS and proinflammatory cytokine production (43). Whether TRIB3 promotes diabetic vascular diseases in a NOX-dependent manner will be an interesting investigation. Catalase, SOD1, GPX1, and GPX4 are a group of key antioxidant enzymes that degrade ROS and protect cells from oxidative stress damage (32). In the current study, antioxidation ability was impaired in TRIB3 MOE mice, as evidenced by significantly decreased expression of catalase, GPX1 and GPX4, but was enhanced in TRIB3 MKO mice, as evidenced by significantly increased expression of catalase, SOD1 and GPX1.

Endoplasmic reticulum stress has been shown to induce TRIB3 expression at the transcription level via the ATF4-CHOP pathway, and TRIB3 in turn acts as a negative feedback regulator of the pathway by suppressing transcriptional activity of CHOP (31,44). In the current study, we observed an increase in muscle ATF4 and CHOP mRNA levels in TRIB3 MOE mice when they consumed normal chow; however, ATF4 remained elevated with high-fat feeding while CHOP was suppressed. The data suggest that TRIB3 can inhibit CHOP expression via an ATF4-independent mechanism.

In summary (Supplementary Fig. 1), TRIB3, as a glucose responsive gene (23,28), acts as a nutrient sensor in muscle, which has been reported in prostate cancer cells, where TRIB3 is regulated by nutrient availability in a phosphatidylinositide 3-kinase–dependent manner (45). With sustained hyperglycemia in diabetes, the development of glucose-induced insulin resistance depends on muscle TRIB3. Thus, TRIB3 appears to be the long-sought-after mediator of insulin resistance that results from increased glucose flux via the HBP pathway. In addition, systemic insulin resistance as a consequence of diet-induced obesity is also dependent on muscle TRIB3. The observations that overexpression of TRIB3 exacerbated, but knockout of TRIB3 prevented, HFD-induced insulin resistance substantiates TRIB3 as a negative regulator of the insulin-signaling pathway under conditions of nutrient excess. In the setting of diabetes and nutrient excess, the induction of insulin resistance by TRIB3 is coupled to changes in multiple mechanistic pathways, including oxidative stress, antioxidants, inflammation, Adq action, endoplasmic reticulum stress, and insulin signal transduction. When mice consumed normal chow, however, muscle TRIB3 influenced energy expenditure and body mass without any change in insulin sensitivity. The data indicate that TRIB3 is a critical regulator of in vivo energy metabolism under physiological conditions as well as a necessary factor in the induction of insulin resistance by nutrient excess. TRIB3 is a novel target for treatment of insulin resistance and glucose toxicity in diabetes.

Funding. This work was supported by grants from the National Institutes of Health (DK-038765 and DK-083562), the Department of Veterans Affairs Merit Review Program, and the American Diabetes Association (1-13-IN-19) and by a grant from the National Institute of Diabetes and Digestive and Kidney Diseases to the UAB Diabetes Research Center Core Facilities (P60 DK079626).

Duality of Interest. No potential conflicts of interest relevant to this article were reported.

Author Contributions. W.Z. designed the study, performed experiments, analyzed the data, and wrote, reviewed, and edited the manuscript. M.W. performed experiments, analyzed data, and reviewed the manuscript. T.K., R.H.J., W.J.G., N.L., M.K., E.M., L.T., and D.S. helped with animal experiments and glucose transport experiments. Q.Y. helped with design and review of the manuscript. Y.F. and W.T.G. designed the study, interpreted the data, and reviewed the manuscript. W.Z. is the guarantor of this work and, as such, had full access to all the data in the study and takes responsibility for the integrity of the data and the accuracy of the data analysis.

Prior Presentation. Parts of this study were presented orally and in poster form at the 74th Scientific Sessions of the American Diabetes Association, San Francisco, CA, 13–17 June 2014, and the 75th Scientific Sessions of the American Diabetes Association, Boston, MA, 5–9 June 2015.

References

1. Garvey W, Birnbaum M. Insulin resistance and disease. In *Bailliere's Clinical Endocrinology and Metabolism*. Ferrannini E, Ed. London, Bailliere Tindall, 1994, p. 785–873

2. Garvey WT, Olefsky JM, Griffin J, Hamman RF, Kolterman OG. The effect of insulin treatment on insulin secretion and insulin action in type II diabetes mellitus. Diabetes 1985;34:222–234

3. Rossetti L, Giaccari A, DeFronzo RA. Glucose toxicity. Diabetes Care 1990; 13:610–630

4. Unger RH, Grundy S. Hyperglycaemia as an inducer as well as a consequence of impaired islet cell function and insulin resistance: implications for the management of diabetes. Diabetologia 1985;28:119–121
5. Friedman JE, Dohm GL, Leggett-Frazier N, et al. Restoration of insulin responsiveness in skeletal muscle of morbidly obese patients after weight loss. Effect on muscle glucose transport and glucose transporter GLUT4. J Clin Invest 1992;89:701–705
6. Greenfield MS, Doberne L, Rosenthal M, Schulz B, Widstrom A, Reaven GM. Effect of sulfonylurea treatment on in vivo insulin secretion and action in patients with non-insulin-dependent diabetes mellitus. Diabetes 1982;31:307–312
7. Kolterman OG, Gray RS, Shapiro G, Scarlett JA, Griffin J, Olefsky JM. The acute and chronic effects of sulfonylurea therapy in type II diabetic subjects. Diabetes 1984;33:346–354
8. Scarlett JA, Kolterman OG, Ciaraldi TP, Kao M, Olefsky JM. Insulin treatment reverses the postreceptor defect in adipocyte 3-O-methylglucose transport in type II diabetes mellitus. J Clin Endocrinol Metab 1983;56:1195–1201
9. Yki-Järvinen H, Helve E, Koivisto VA. Hyperglycemia decreases glucose uptake in type I diabetes. Diabetes 1987;36:892–896
10. Karnieli E, Armoni M, Cohen P, Kanter Y, Rafaeloff R. Reversal of insulin resistance in diabetic rat adipocytes by insulin therapy. Restoration of pool of glucose transporters and enhancement of glucose-transport activity. Diabetes 1987;36:925–931
11. Rossetti L, Smith D, Shulman GI, Papachristou D, DeFronzo RA. Correction of hyperglycemia with phlorizin normalizes tissue sensitivity to insulin in diabetic rats. J Clin Invest 1987;79:1510–1515
12. Richter EA, Hansen BF, Hansen SA. Glucose-induced insulin resistance of skeletal-muscle glucose transport and uptake. Biochem J 1988;252:733–737
13. Garvey WT, Olefsky JM, Matthaei S, Marshall S. Glucose and insulin coregulate the glucose transport system in primary cultured adipocytes. A new mechanism of insulin resistance. J Biol Chem 1987;262:189–197
14. Bailey CJ, Turner SL. Glucosamine-induced insulin resistance in L6 muscle cells. Diabetes Obes Metab 2004;6:293–298
15. Baron AD, Zhu JS, Zhu JH, Weldon H, Maianu L, Garvey WT. Glucosamine induces insulin resistance in vivo by affecting GLUT 4 translocation in skeletal muscle. Implications for glucose toxicity. J Clin Invest 1995;96:2792–2801
16. Cooksey RC, Hebert LF Jr, Zhu JH, Wofford P, Garvey WT, McClain DA. Mechanism of hexosamine-induced insulin resistance in transgenic mice overexpressing glutamine:fructose-6-phosphate amidotransferase: decreased glucose transporter GLUT4 translocation and reversal by treatment with thiazolidinedione. Endocrinology 1999;140:1151–1157
17. Marshall S, Bacote V, Traxinger RR. Discovery of a metabolic pathway mediating glucose-induced desensitization of the glucose transport system. Role of hexosamine biosynthesis in the induction of insulin resistance. J Biol Chem 1991;266:4706–4712
18. Marshall S. Role of insulin, adipocyte hormones, and nutrient-sensing pathways in regulating fuel metabolism and energy homeostasis: a nutritional perspective of diabetes, obesity, and cancer. Sci STKE 2006;2006:re7
19. Traxinger RR, Marshall S. Coordinated regulation of glutamine:fructose-6-phosphate amidotransferase activity by insulin, glucose, and glutamine. Role of hexosamine biosynthesis in enzyme regulation. J Biol Chem 1991;266:10148–10154
20. Marshall S, Bacote V, Traxinger RR. Complete inhibition of glucose-induced desensitization of the glucose transport system by inhibitors of mRNA synthesis. Evidence for rapid turnover of glutamine:fructose-6-phosphate amidotransferase. J Biol Chem 1991;266:10155–10161
21. Du K, Herzig S, Kulkarni RN, Montminy M. TRB3: a tribbles homolog that inhibits Akt/PKB activation by insulin in liver. Science 2003;300:1574–1577
22. Prudente S, Sesti G, Pandolfi A, Andreozzi F, Consoli A, Trischitta V. The mammalian tribbles homolog TRIB3, glucose homeostasis, and cardiovascular diseases. Endocr Rev 2012;33:526–546
23. Liu J, Zhang W, Chuang GC, et al. Role of TRIB3 in regulation of insulin sensitivity and nutrient metabolism during short-term fasting and nutrient excess. Am J Physiol Endocrinol Metab 2012;303:E908–E916
24. Qi L, Heredia JE, Altarejos JY, et al. TRB3 links the E3 ubiquitin ligase COP1 to lipid metabolism. Science 2006;312:1763–1766
25. Wu X, Wang J, Cui X, et al. The effect of insulin on expression of genes and biochemical pathways in human skeletal muscle. Endocrine 2007;31:5–17
26. Wu X, Patki A, Lara-Castro C, et al. Genes and biochemical pathways in human skeletal muscle affecting resting energy expenditure and fuel partitioning. J Appl Physiol (1985) 2011;110:746–755
27. Liu J, Wu X, Franklin JL, et al. Mammalian Tribbles homolog 3 impairs insulin action in skeletal muscle: role in glucose-induced insulin resistance. Am J Physiol Endocrinol Metab 2010;298:E565–E576
28. Zhang W, Liu J, Tian L, Liu Q, Fu Y, Garvey WT. TRIB3 mediates glucose-induced insulin resistance via a mechanism that requires the hexosamine biosynthetic pathway. Diabetes 2013;62:4192–4200
29. Kim KH, Jeong YT, Oh H, et al. Autophagy deficiency leads to protection from obesity and insulin resistance by inducing Fgf21 as a mitokine. Nat Med 2013;19:83–92
30. Sano H, Kane S, Sano E, et al. Insulin-stimulated phosphorylation of a Rab GTPase-activating protein regulates GLUT4 translocation. J Biol Chem 2003;278:14599–14602
31. Ohoka N, Yoshii S, Hattori T, Onozaki K, Hayashi H. TRB3, a novel ER stress-inducible gene, is induced via ATF4-CHOP pathway and is involved in cell death. EMBO J 2005;24:1243–1255
32. Kang DH, Kang SW. Targeting cellular antioxidant enzymes for treating atherosclerotic vascular disease. Biomol Ther (Seoul) 2013;21:89–96
33. Wu X, Patki A, Lara-Castro C, et al. Genes and biochemical pathways in human skeletal muscle affecting resting energy expenditure and fuel partitioning. J Appl Physiol (1985) 2011;110:746–755
34. Lara-Castro C, Fu Y, Chung BH, Garvey WT. Adiponectin and the metabolic syndrome: mechanisms mediating risk for metabolic and cardiovascular disease. Curr Opin Lipidol 2007;18:263–270
35. Fu Y, Luo N, Klein RL, Garvey WT. Adiponectin promotes adipocyte differentiation, insulin sensitivity, and lipid accumulation. J Lipid Res 2005;46:1369–1379
36. Hong EG, Ko HJ, Cho YR, et al. Interleukin-10 prevents diet-induced insulin resistance by attenuating macrophage and cytokine response in skeletal muscle. Diabetes 2009;58:2525–2535
37. Bilan PJ, Samokhvalov V, Koshkina A, Schertzer JD, Samaan MC, Klip A. Direct and macrophage-mediated actions of fatty acids causing insulin resistance in muscle cells. Arch Physiol Biochem 2009;115:176–190
38. Sorescu D, Weiss D, Lassègue B, et al. Superoxide production and expression of nox family proteins in human atherosclerosis. Circulation 2002;105:1429–1435
39. Inoguchi T, Nawata H. NAD(P)H oxidase activation: a potential target mechanism for diabetic vascular complications, progressive beta-cell dysfunction and metabolic syndrome. Curr Drug Targets 2005;6:495–501
40. Morse E, Schroth J, You YH, et al. TRB3 is stimulated in diabetic kidneys, regulated by the ER stress marker CHOP, and is a suppressor of podocyte MCP-1. Am J Physiol Renal Physiol 2010;299:F965–F972
41. Martins AR, Nachbar RT, Gorjao R, et al. Mechanisms underlying skeletal muscle insulin resistance induced by fatty acids: importance of the mitochondrial function. Lipids Health Dis 2012;11:30
42. Dikalova A, Clempus R, Lassègue B, et al. Nox1 overexpression potentiates angiotensin II-induced hypertension and vascular smooth muscle hypertrophy in transgenic mice. Circulation 2005;112:2668–2676
43. Gray SP, Di Marco E, Okabe J, et al. NADPH oxidase 1 plays a key role in diabetes mellitus-accelerated atherosclerosis. Circulation 2013;127:1888–1902
44. Jousse C, Deval C, Maurin AC, et al. TRB3 inhibits the transcriptional activation of stress-regulated genes by a negative feedback on the ATF4 pathway. J Biol Chem 2007;282:15851–15861
45. Schwarzer R, Dames S, Tondera D, Klippel A, Kaufmann J. TRB3 is a PI 3-kinase dependent indicator for nutrient starvation. Cell Signal 2006;18:899–909